Constraining oceanic dust deposition using surface ocean dissolved Al

Qin Han,[1] J. Keith Moore,[1] Charles Zender,[1] Chris Measures,[1] and David Hydes[1]

Received 16 March 2007; revised 9 November 2007; accepted 7 December 2007; published 12 April 2008.

[1] We use measurements of ocean surface dissolved Al, a global Biogeochemical Elemental Cycling (BEC) ocean model, and the global Dust Entrainment and Deposition (DEAD) model to constrain dust deposition to the oceans. Our Al database contains all available measurements with best coverage in the Atlantic. Vertical profiles and seasonal data exist in limited regions. Observations show that surface dissolved Al is distributed similarly to the dust deposition predicted by DEAD and other models. There is an equatorial Atlantic Al maximum that decreases toward higher latitudes. There are high Al concentrations in the Mediterranean Sea and the Arabian Sea and low concentrations in the Pacific and the Southern Ocean. The ocean basins maintain more distinct Al profiles than Fe profiles in the upper ocean, consistent with a weaker biological influence on Al than Fe. The BEC-predicted surface dissolved Al compares relatively well with observations. The Al distribution reflects the combined effects of Al input from dust and Al removal by particle scavenging and biological uptake by diatoms. Model-observed biases suggest a southward shift of maximum dust deposition compared to current dust model predictions. DEAD appears to overestimate deposition north of 30°N in the Pacific and to underestimate deposition south of 30°N. Observed Al concentrations and the ocean model–predicted surface Al lifetime provide a semi-independent method to estimate oceanic dust deposition. This technique indicates that DEAD may overestimate dust deposition to the north equatorial Atlantic but underestimate in other Atlantic regions, the Southern Ocean, and the Arabian Sea. However, spatial variations in aerosol Al solubility may also contribute to the model-observation mismatch. Our results have implications for all dust-borne ocean nutrients including Fe and demonstrate the potential of marine geochemical data to constrain atmospheric aerosol deposition fields.

Citation: Han, Q., J. K. Moore, C. Zender, C. Measures, and D. Hydes (2008), Constraining oceanic dust deposition using surface ocean dissolved Al, *Global Biogeochem. Cycles*, *22*, GB2003, doi:10.1029/2007GB002975.

1. Introduction

[2] Atmospheric aerosols deliver terrestrial elements essential to the ocean ecosystem and ocean biogeochemical cycles and thus have an important impact on the global carbon cycle. Aerosol-borne nutrients that can limit the growth of phytoplankton include nitrate, ammonium, phosphate, silicate and iron. Iron deficiency limits the primary production in High-Nutrient Low-Chlorophyll (HNLC) ocean areas [*Martin and Fitzwater*, 1988] and most iron in the remote ocean comes from mineral dust deposition [*Fung et al.*, 2000]. Unfortunately, aerosol deposition to the surface ocean is poorly quantified because of sparse measurements [*Prospero*, 1996]. Dissolved Al provides an independent estimate for atmospheric mineral dust aerosol deposition [*Measures and Brown*, 1996; *Gehlen et al.*, 2003]. Direct measurements of oceanic Al or dust deposition are only available at a handful of remote islands for limited time periods [*Duce et al.*, 1991; *Prospero*, 1996; *Ginoux et al.*, 2001]. Estimates of ocean nutrient deposition are extrapolated from these observations or predicted by atmospheric models which have been evaluated against available concentration and optical depth data [*Andersen et al.*, 1998; *Mahowald et al.*, 1999; *Ginoux et al.*, 2001; *Zender et al.*, 2003]. The intermodel uncertainty in global deposition estimates is at least a factor of four [*Zender et al.*, 2004]. Deposition uncertainty propagates into uncertainties in oceanic iron availability and in atmospheric aerosol direct and indirect radiative forcing. To better understand the role of aerosol deposition on ocean biogeochemistry and the global carbon cycle, dust input to the ocean must be better constrained.

[3] Aluminum is an ideal tracer for quantifying the dust deposition to the surface ocean because of its geochemical characteristics. First, Al is a major and relatively invariant

[1]Department of Earth System Science, University of California, Irvine, Irvine, California, USA.

0886-6236/08/2007GB002975$12.00

component of continental materials [*Wedephohl*, 1995]. Al is the third most common element in continental materials accounting for about 8% of crustal mass. Second, the residence time of Al in the surface ocean is relatively short (~6.5 years) [*Jickells et al.*, 1994] which impedes transfer from the coastal areas to the open oceans. That means the atmospheric input is the main source for the surface ocean Al concentration in the remote oceans. Third, ocean Al chemistry is relatively simple compared to Fe because Al is not involved in complicated redox chemistry.

[4] The concentrations and distributions of trace metals in the ocean are controlled by processes including external input, removal, and internal cycling. It is likely that Al cycles in a manner similar to Fe in the oceans [*Bruland and Lohan*, 2003]. The most important source for iron and aluminum is partial dissolution from dust deposition. Al solubility estimates range widely from 0.5–86% with a mean of about 5% [*Prospero et al.*, 1987; *Sato*, 2003; *Baker et al.*, 2006]. Removal processes include active biological uptake by diatoms and passive scavenging onto particles. The removal rate is first-order dependent on the particle concentration [*Moran et al.*, 1992]. There is some active uptake and incorporation into the frustules by diatoms [*Gehlen et al.*, 2002]. According to the few deposition observations available, the dissolved Al distribution seems well correlated to the oceanic dust flux [*Measures and Vink*, 2000]. Typical surface Al concentrations range from 50 to 0.1 nM for high-dust areas and low-dust areas respectively [*Measures and Vink*, 2000]. *Measures and Vink* [2000] used a simple model named MADCOW to invert observed Al concentrations to dust deposition fluxes. MADCOW assumes that dissolved Al is in steady state, that surface Al originates only from partial dissolution of deposited mineral dust, and that the Al loss occurs solely from biological particle scavenging. In addition, a constant mixed layer depth and residence time for dissolved Al are assumed. With these assumptions, Al scavenging balances the partial dissolution of deposited Al. MADCOW-inferred dust deposition from surface Al concentrations agrees fairly well with observations [*Duce et al.*, 1991] over 4 orders of magnitude [*Measures and Vink*, 2000].

[5] *Gehlen et al.* [2003] assembled a database for dissolved Al concentrations in oceanic water and used a geochemical ocean general circulation model coupled with the geochemical cycles of Al and Si to study the relationship between surface Al and total dust input. They provided an empirically corrected parameterization of the partition coefficient for Al removal by biogenic opal and they left the Al scavenging rate a free parameter. Their ocean model–calculated Al concentration in the surface ocean from two different modeled dust deposition fields [*Andersen et al.*, 1998; *Mahowald et al.*, 1999]. They obtained the best fit between predicted and measured Al concentrations using an Al solubility of 1.5%–3.0%. Their work demonstrates how ocean observations may be used to evaluate atmospheric model estimates of mineral aerosol deposition. The many uncertainties involved in inferring dust deposition from Al measurements include the choice of scavenging parameters, Al solubility, and the surface ocean biology, which itself through Fe addition may depend on dust deposition.

[6] We use an augmented Al observational database that is used to characterize, evaluate, and improve our understanding of ocean Al cycling as represented in a state-of-the-art ocean ecosystem-biogeochemical model. We have assembled all known, relevant oceanic dissolved Al observations into a single database. The database includes eighteen more cruise tracks and stations and approximately 3 times as much data (10,460 points) as previous studies [*Gehlen et al.*, 2003]. The newer data significantly improves the characterization of the North Pacific and Southern Ocean Al cycle. Second, we develop a more realistic and complete prognostic global ocean Al cycle model which agrees well overall with the measurements. The model provides new insights on the timescale, solubility, and basin distributions of Al that are consistent with measurements.

2. Methods

2.1. Database of Dissolved Al Observations

[7] The concentration of dissolved Al in the oceans has been measured during approximately forty cruises and stations since 1976. Our augmented database includes virtually all Al data published since 1979, as well as unpublished data from C. Measures and D. Hydes (see Table 1). There are 10,460 data points in all.

[8] *Gehlen et al.* [2003] collated data from 12 cruises and stations. These and the 18 newer cruise tracks are plotted in Figure 1. Much more data will become available in the near future through sampling on cruises associated with the CLIVAR and GEOTRACES programs. These data will include observations from the cruise tracks across the Pacific and the Indian oceans and they will help to fill large data gaps in these ocean regions. At the global ocean scale, most regions are still poorly observed. The Atlantic coverage is best, especially the equatorial Atlantic, where dust input is high because of emissions from North African deserts. Most measurements are limited to the surface ocean and only 20% of data are beneath 100 m. There are several transects across the North Pacific. Some data are available in the HNLC (high-nutrient, low- chlorophyll) region of the Southern Ocean and around Southeast Asia. In limited regions, e.g., the Hawaii Ocean Time-series (HOT), Bermuda Atlantic Time-series (BATS), Arabian Sea, the data are sufficient to describe the seasonal variability.

[9] The original batch fluorimetric method for measuring Al using the reagent Lumogallion was developed by *Hydes and Liss* [1976]. This method has a detection limit of 2 nM of aluminum and has been used in the relatively high concentration region of the Atlantic Ocean. The Flow Injection Analysis (FIA) version of this method has a detection limit of 0.6 nM and has been used in various ocean basins. Methods that can be used on even lower values were applied successfully after that: the method using atomic absorption achieved the best detection limits of 0.1 nM [*Orians and Bruland*, 1986] and the gas chromatography method can be used at levels between 0.6 and 120 nM [*Measures and Edmond*, 1989]. There is no apparent discrepancy among these methods [*Orians and Bruland*, 1986; *Measures et al.*, 1986].

Table 1. Sources of Dissolved Al Measurements

Cruises or Locations	Dates	Source
Atlantic		
EN107	Nov 1983	*Measures et al.* [1984]
Meteor60	3 Mar to 19 Apr 1982	*Kremling* [1985]
SAVE	28 Jan to 7 Mar 1988	*Measures and Edmond* [1990]
IOC90	Mar 1990	*Measures* [1995]
IOC96	18 May to 20 Jun 1996	*Vink and Measures* [2001]
Discovery125	31 Jan to 26 Feb 1982	*Hydes* [1983]
IOC93	Aug 1993	*Hall and Measures* [1998]
EN120	Aug–Sep 1984	*Measures et al.* [1986]
AMT-3	22 Sep to 25 Oct 1996	*Bowie et al.* [2002]
AMT-6	15 May to 14 Jun 1998	*Bowie et al.* [2002]
ANT VIII	1–29 May 1990	*Helmers and van der Loeff* [1993]
ANT IX	19 Oct to 14 Nov 1990	*Helmers and van der Loeff* [1993]
A16NR	20 Jun to 8 Aug 2003	Measures
WBEX	May 1986	Measures
K69/10	Oct 1977	*Hydes* [1979]
EN157	Mar 1987	Measures
BATS	1983–1985	*Jickells* [1986]
Bermuda	Apr 1977	*Stoffyn and Mackenzie* [1982]
Barbados	Jul 1977	*Stoffyn and Mackenzie* [1982]
R.V. Pelagia	3–29 Oct 2002	*Kramer et al.* [2004]
Darwin cruise 50	11–20 Jul, 1990	Hydes
BOFS/OMEX/LOIS	Jan 1994 and May 1995	Hydes
Pacific		
MC-80	Sep–Oct 1980	*Orians and Bruland* [1985]
VERTEX-4	Jul 1983	*Orians and Bruland* [1985]
VERTEX-5	Jun–Jul 1984	*Orians and Bruland* [1985]
MBARI SOLAS	Mar–May 2001	*Johnson et al.* [2003]
IOC2002	1 May to 5 Jun 2002	*Measures et al.* [2005]
HOT	1994–1997	Measures
Southern Ocean		
Southern Ocean process study	Oct 1994 to Jan 1996	U.S. JGOFS database
Stena Arctica	Jan 1989	*Moran et al.* [1992]
Weddell Sea	Feb–Mar 1991	*Sanudo-Wilhelmy et al.* [2002]
Indian Ocean		
Arabian Sea process study	8 Jan to 24 Dec 1995	*Measures and Vink* [1999]
R.V. Hakuho-maru	Jul 1996	*Obata et al.* [2004]
ORVSKC-34	Jul–Aug 1987	*Narvekar and Singbal* [1993]
ORVSKC-47	Nov–Dec 1988	*Narvekar and Singbal* [1993]
ORVSCK-38[a]	Jan–Feb 1988	*Upadhyay and Gupta* [1994]
Mediterranean Sea		
Anoxic Basins Cruise	21 May to 5 Jun 1987	*Hydes et al.* [1988]
Corsica	20 Sep 1976 and 30 May 1977	*Stoffyn and Mackenzie* [1982]
Western and eastern Mediterranean	Apr 1988	*Brown et al.* [1992]
EROS2000 program[a]	Dec 1988 to Jul 1993	*Chou and Wollast* [1997]
Station RSMO[a]	Sep 1976 to Aug 1977	*Caschetto and Wollast* [1979]

[a]The original data are not included in the published paper nor in our research.

[10] Most of the data in Table 1 were obtained from filtered samples, some though were from unfiltered samples. However, the dissolution of particulate Al is negligible if the storage time is minimal and the samples are not acidified [*Measures et al.*, 1986]. Also, the unfiltered data are consistent with those filtered [*Bowie et al.*, 2002].

2.2. Global Biogeochemical Model

[11] In this study, we incorporated ocean Al cycling in the Biogeochemical Elemental Cycling (BEC) ocean model [*Moore et al.*, 2004]. The BEC ocean model couples the upper ocean ecosystem model [*Moore et al.*, 2002] and an expanded biogeochemistry module [*Doney et al.*, 2003] with the ocean circulation component of the Community Climate System Model 3.0 [*Collins et al.*, 2006]. This marine ecosystem model includes one zooplankton and four phytoplankton functional groups: coccolithophores, small phytoplankton, diatoms, and diazotrophs; key limiting nutrients: nitrate, ammonium, phosphate, iron, and silicate; sinking particulates and dissolved organic matter. In these components, the model tracks carbon, nitrogen, phosphorus, iron, silicon, oxygen and calcium carbonate and then predicts the biomass, productivity, community structure, and carbon export in the ocean ecosystem.

[12] This coupled model accurately predicts the HNLC regions in the Southern Ocean and subarctic Pacific Ocean, with a larger than observed spatial extent of HNLC conditions in the equatorial Pacific region, which is a common problem in coarse resolution models [*Moore et al.*, 2004]. It also reproduces known basin-scale patterns of primary production, export productions and macronutrient concentrations. The BEC model realistically simulates the biogenic silica production as well as the ocean circulation (e.g., mixed layer depth, element transport) which helps us estimate dust deposition from dissolved Al. Sensitivity tests indicate that the model response to variations in atmospher-

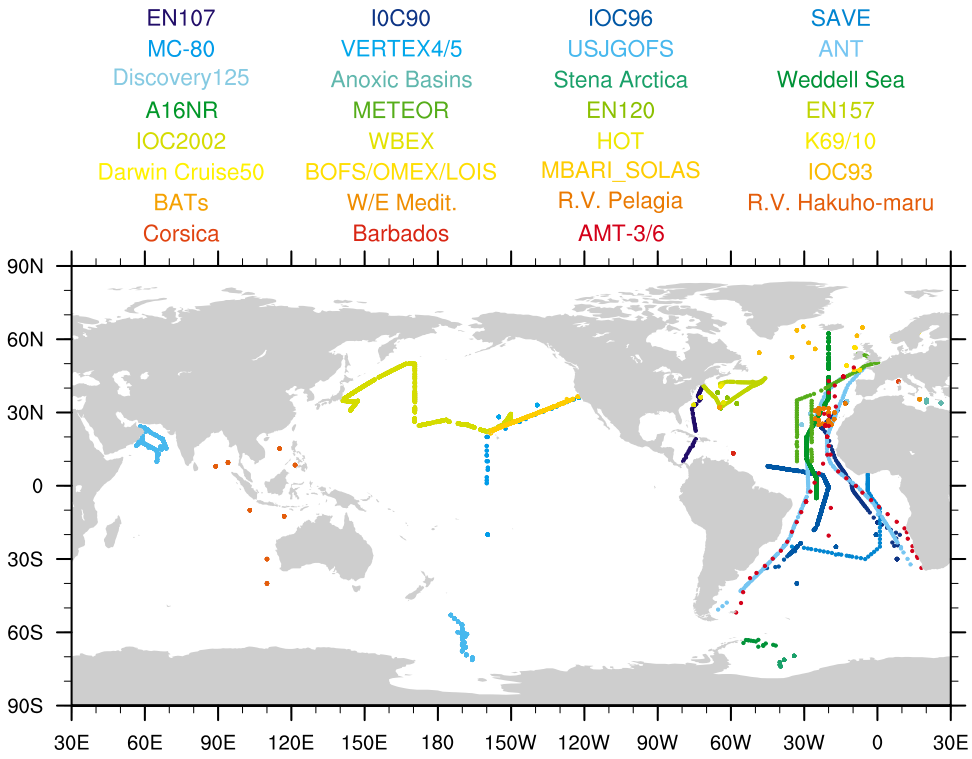

Figure 1. Individual cruise tracks. Compare to *Gehlen et al.* [2003, Figure 2a].

ic dust input is realistic compared to field experiments [*Moore et al.*, 2004, 2006; *Krishnamurthy et al.*, 2008]. This indicates that this model is appropriate for studying the relationship between atmospheric dust input and ocean Al concentration. The BEC model employed here includes some parameter modifications described by *Krishnamurthy et al.* [2008].

[13] We incorporated a dissolved Al tracer in the BEC model largely following the parameterizations developed for iron. Partial dissolution of deposited dust provides Al to the ocean and particle scavenging removes it. For our standard simulation we assume a constant Al/dust weight ratio of 8% and a constant solubility for the Al of 5%. We include a sensitivity experiment to indicate how this assumed solubility impacts our results. Other processes simulated in the Al cycle include biological uptake by diatoms, remineralization, and advection and mixing, due to ocean physics. The diatom Al/Si uptake ratio is a function of ambient Al and Si concentrations, based on the relationship found by *Gehlen et al.* [2002] (see Appendix A for details). Following the ballast mineral model which relates the ballast mineral flux to the POC flux [*Armstrong et al.*, 2002], our model ties Al remineralization to the POC remineralization, which is a good proxy for the total sinking particle flux in the model. According to the ballast mineral model, there are two kinds of sinking particles: easily remineralized and hardly remineralized, which refer to the soft and hard fluxes described by *Armstrong et al.* [2002]. The full model details and the parameterizations for the control run are given in Appendix A.

[14] The Dust Entrainment And Deposition (DEAD) model [*Zender et al.*, 2003] provides the dust deposition input field for the BEC model. The DEAD model simulates size-dependent dust processes including mobilization, transport, and dry and wet deposition for particles size from 0.1–10 μm which includes most long-range transported dust. The predicted and observed climatological mean dust deposition flux are compared at 6 oceanic stations, including Oahu [*Zender et al.*, 2003] which is near HOT. The predictions of DEAD for LGM, preindustrial, current, and doubled CO_2 climates are evaluated against available observations given by *Mahowald et al.* [2006]. Here we use the monthly mean dust deposition field obtained from driving DEAD with 1990s observed meteorology [*Zender et al.*, 2003]. A constant solubility of 5% for both Al and Fe is assumed upon deposition.

3. Results

3.1. Observed Al Climatology

[15] The observed Al concentrations show clear regional trends with depth at the basin scale (Figure 2a and Figure S1[1]). The highest and next highest Al concentrations are in the Mediterranean Sea and Atlantic Ocean, respectively. Interestingly, the Al concentration near the bottom of the Mediterranean Sea decreases sharply. The Al concentration below the brine interface drops by an order of magnitude and is similar to the observations in the North Atlantic. These data are reported by *Hydes et al.* [1988] who think the clay mineral formation process may explain this low Al concentration. The Southern Ocean and the Pacific Ocean have very low Al concentrations. The mean subsur-

[1]Auxiliary materials are available in the HTML. doi:10.1029/2007GB002975.

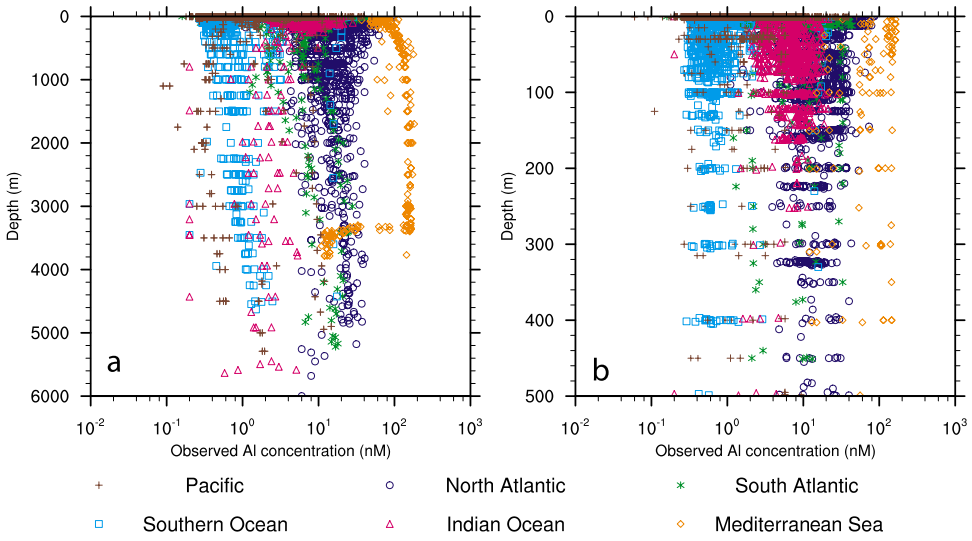

Figure 2. Dissolved Al concentrations in different ocean basins: (a) 0–6000 m; (b) 0–500 m.

face ocean (150–500 m) and surface ocean (0–50 m) concentrations are tabulated by basin in Table 2. The Al profiles in each basin are very similar throughout the water column except in the Mediterranean (Figure 2b), and vary similarly to the input dust flux from DEAD model simulations. There is a strong correlation between mean DEAD simulated dust deposition and observed mean Al concentrations at the basin scale (r^2 of 0.93 for surface Al and 0.88 for subsurface Al). The consistency of the profiles of Al with depth (Figure 2) and the correlation with estimated dust inputs (Table 2) suggest that dissolved Al is a good proxy for dust deposition.

[16] The surface layer (0–50 m) Al data are averaged onto the global model grid (Figure 3a). Data are averaged unweighted where there are multiple points in one grid cell. The distribution of surface dissolved Al is very similar to the distribution of modeled dust deposition with a maximum in the equatorial Atlantic, decreasing to higher latitudes. There are high concentrations in the Mediterranean and Arabian seas, and low concentrations in the Pacific and Southern oceans. We reversed the MADCOW model [*Measures and Vink*, 2000] to use the dust deposition field from the DEAD model [*Zender et al.*, 2003] to predict the surface Al concentration (Figure 3b). Since MADCOW relates the dust deposition flux to surface ocean Al concentration by assuming a steady state, a constant Al residence time, a fixed mixed layer depth, and no advection, we can invert MADCOW to estimate Al concentration from the model-predicted dust deposition field. The estimated Al correlates relatively well with the observations although there are significant regional biases (Figure 4a). The inferred Al concentration is systematically too high in the Pacific and in the Arabian Sea, and too low in the South Atlantic. The global averaged Al concentration from MADCOW is 37.95 nM, which is more than 100% larger compare to the observation mean of 18.39 nM. As shown below, our more realistic model with dynamic mixed layer depths and variable Al residence times, significantly reduces these biases.

3.2. Comparison of Observed Al Distributions With the BEC Simulation

[17] The BEC model predicts the dissolved Al distribution that results from the prescribed Al input (via dust) from the DEAD model and removal by prognostic ocean circulation and ecosystem dynamics and particle scavenging. The resulting BEC-predicted surface Al distribution agrees relatively well with observations (Figures 4b, 5, and 6) and captures the equatorial Atlantic maximum, with lower concentrations in the Pacific and Southern oceans. The BEC-predicted Al concentrations averaged by basins compare well with the observations at both the surface and the subsurface ocean (Table 2). In this paper, for the sake of constraining dust deposition, we focus mainly on surface and

Table 2. Mean Al Concentrations at Surface (0–50 m) and Subsurface (150–500 m) Ocean Averaged by Basin[a]

Basin	Dust Deposition Flux ($g\ m^{-2}\ a^{-1}$)	Observed Surface Ocean (nM)	Modeled Surface Ocean (nM)	Observed Subsurface Ocean (nM)	Modeled Subsurface Ocean (nM)
North Atlantic	3.88	23.55	33.56	14.96	14.62
South Atlantic	0.69	15.76	15.33	6.80	4.778
Pacific	0.25	3.07	2.07	3.15	1.39
Southern Ocean	0.29	2.23	1.44	2.38	0.90
Indian Ocean	0.83	15.03	12.82	7.46	6.42
Mediterranean Sea	5.96	65.15	150.3	97.45	102.29

[a]Dust deposition flux comes from DEAD model.

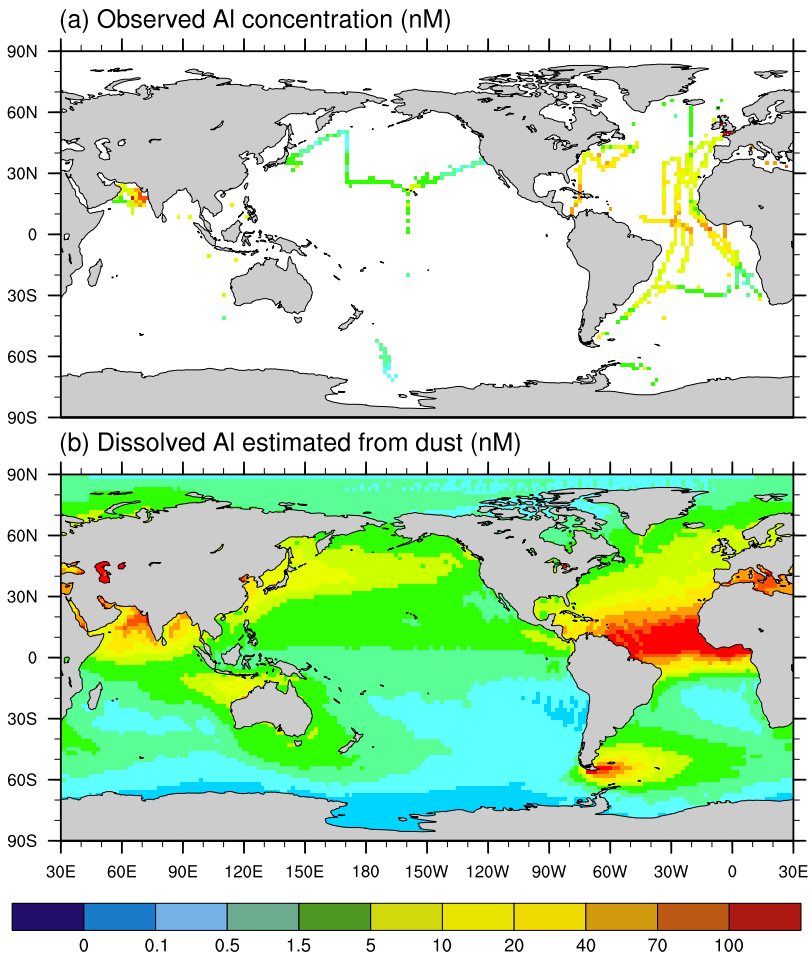

Figure 3. Dissolved Al concentration in surface oceans (0–50 m) from (a) observations and (b) reversed MADCOW/DEAD model and dust deposition field.

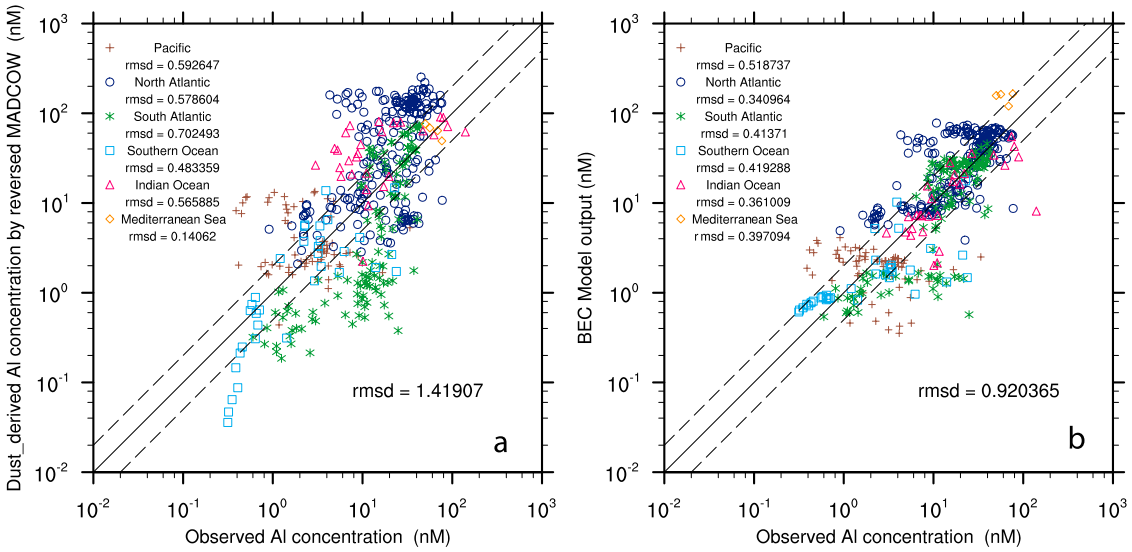

Figure 4. Comparison of surface ocean (0–50 m) Al concentrations between observations and two models: (a) reversed MADCOW/DEAD; (b) BEC/DEAD. Rmsd means root mean square difference, after logarithm transformation.

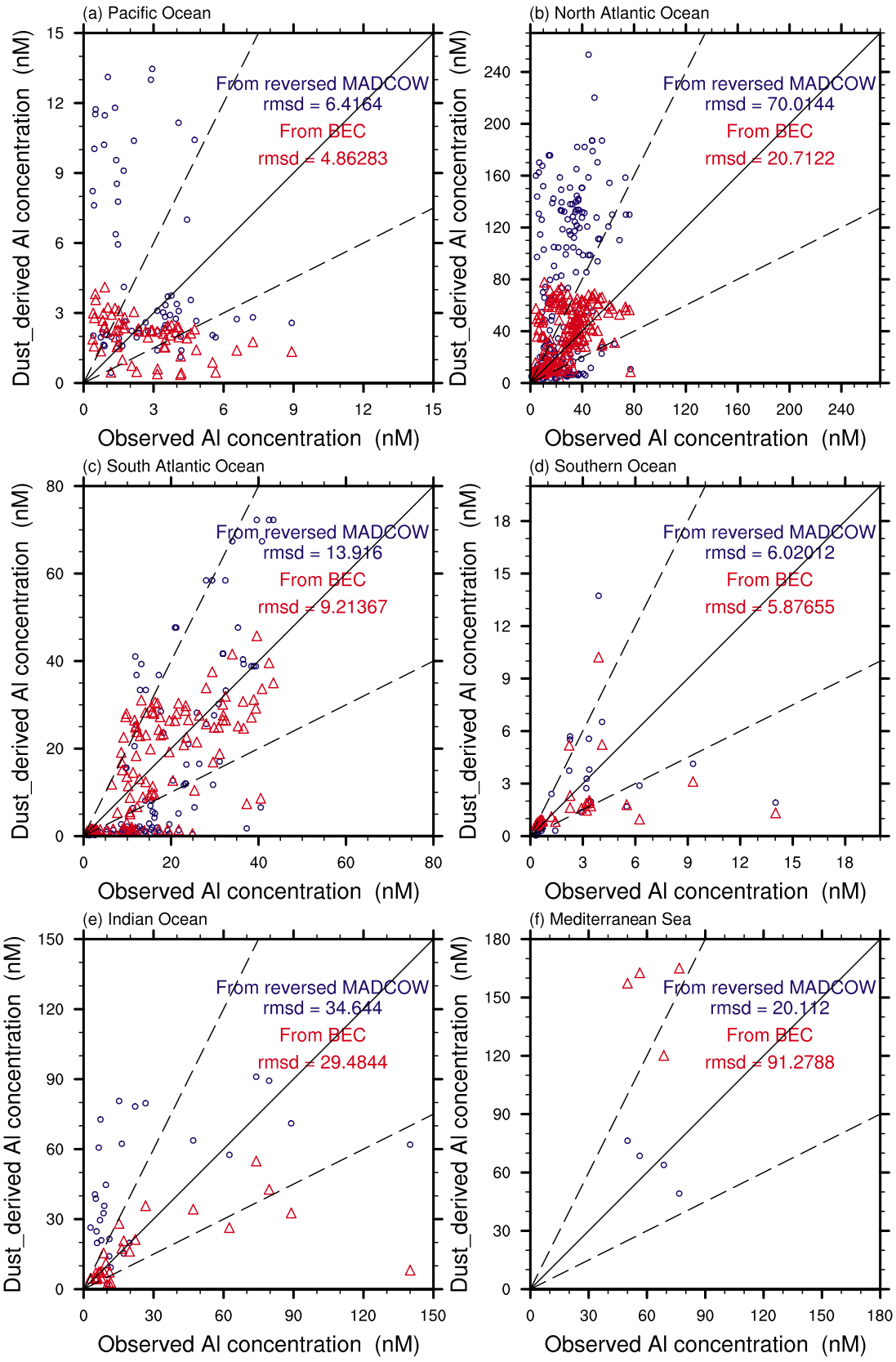
(a) Pacific Ocean
From reversed MADCOW
rmsd = 6.4164
From BEC
rmsd = 4.86283
(b) North Atlantic Ocean
From reversed MADCOW
rmsd = 70.0144
From BEC
rmsd = 20.7122
(c) South Atlantic Ocean
From reversed MADCOW
rmsd = 13.916
From BEC
rmsd = 9.21367
(d) Southern Ocean
From reversed MADCOW
rmsd = 6.02012
From BEC
rmsd = 5.87655
(e) Indian Ocean
From reversed MADCOW
rmsd = 34.644
From BEC
rmsd = 29.4844
(f) Mediterranean Sea
From reversed MADCOW
rmsd = 20.112
From BEC
rmsd = 91.2788
Dust_derived Al concentration (nM)
Observed Al concentration (nM)

Figure 5

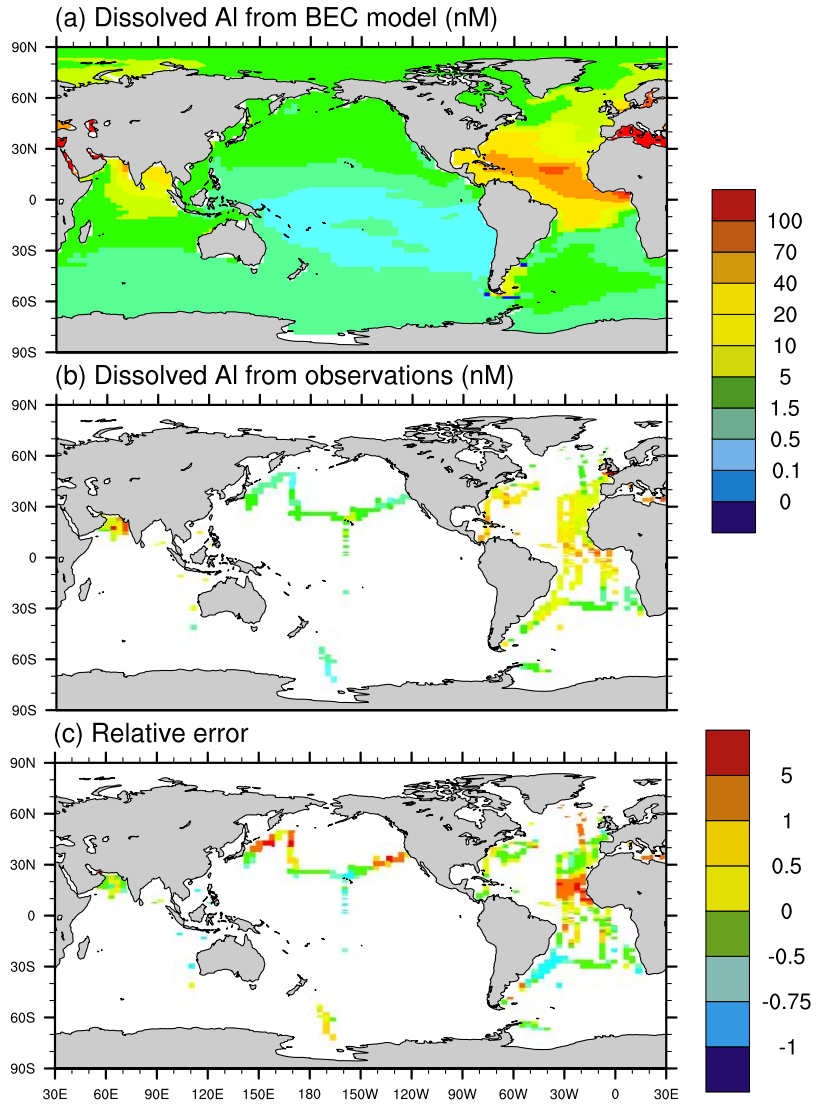

Figure 6. (a) Dissolved Al in surface ocean (0–50 m) from model results. (b) Dissolved Al in surface ocean from observations. (c) Relative error of model: (model-observation)/observation.

upper ocean Al and inferred dust budgets rather than deep ocean Al. The combined models produce large differences in some regions (Figures 5 and 6). The predicted maximum at the North Atlantic is too far north (Figure 6). Biological production and export are underestimated by the model in the Sargasso Sea [*Moore et al.*, 2004]. Thus, the production of particles and scavenging of Al may also be underestimated in this region. The model tends to overestimate Al north of 30°N in the Pacific and to underestimate Al south of it. These biases may arise several ways: (1) the BEC model itself, including the parameterization of production, remineralization and scavenging; (2) the input dust field, which we intend to constrain; (3) the geographic variation of Al concentration in the upper soil; and (4) the Al solubility in the atmospheric aerosols. Sampling biases in the Al data cannot be ruled out. In most regions we are forced to compare climatological mean model predictions to Al data sampled at a particular location on a single day.

[18] The BEC-DEAD model Al predictions are significantly improved relative to MADCOW-DEAD predictions at most regions (compare Figures 4a and 4b). Most BEC-DEAD predictions are within a factor of two of observations. The global averaged Al concentration from BEC is 22.00 nM, much more closer to the mean of observations. The root mean square difference (rmsd, after logarithm transformation) is reduced by 35%. The regional biases in the Pacific Ocean, the Arabian Sea, North Atlantic Ocean and South Atlantic Ocean have also been greatly reduced

Figure 5. Comparison of surface ocean (0–50 m) Al concentrations between observations and two models at different ocean basins: (a) Pacific Ocean, (b) North Atlantic Ocean, (c) South Atlantic Ocean, (d) Southern Ocean, (e) Indian Ocean, and (f) Mediterranean Sea. Blue for reversed MADCOW/DEAD and red for BEC/DEAD. Rmsd means root mean square difference.

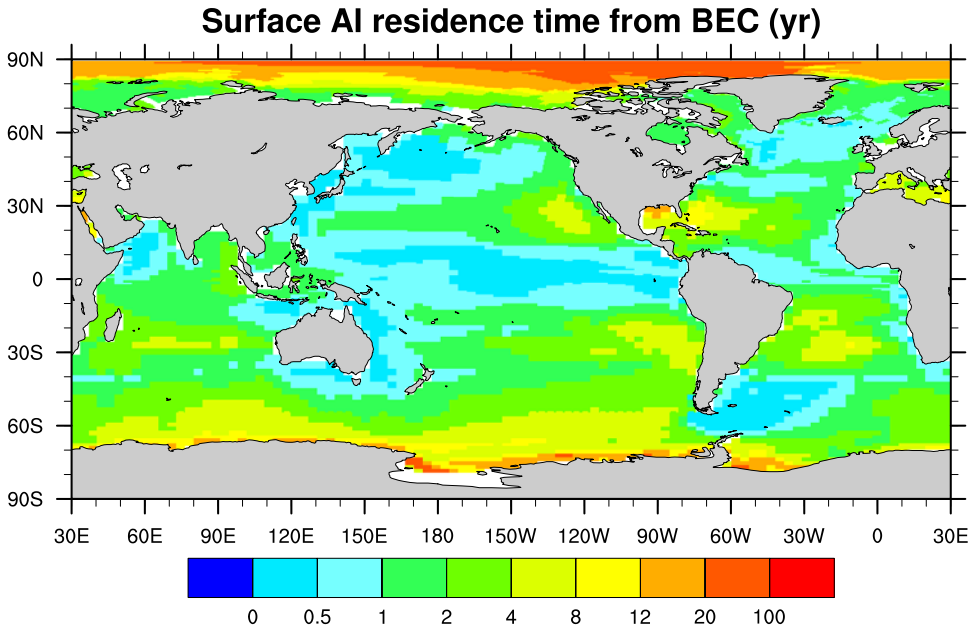

Figure 7. Modeled residence time of surface ocean (0–50 m) dissolved Al.

(Figure 5; note the reduction in rmsd and the different scales for each ocean basin). Relative to MADCOW, the BEC model predicts longer residence times in the South Atlantic and shorter residence times in the Arabian Sea and most regions of the North Atlantic Ocean. This variable Al residence time partly explains the improved results in these regions. Remaining biases include overestimates in the North Atlantic and underestimations in the South Atlantic. These biases are most likely due to errors in either dust inputs or our assumed solubility. The BEC model actually is worse than MADCOW in the Mediterranean Sea (Figure 5f), which is probably due to the assumed solubility, similar to the high-dust area of North Atlantic. The BEC has a smaller root mean square difference in all other regions (Figure 5).

[19] Our ocean biogeochemistry ecosystem model and Al cycle are more complex than MADCOW [*Measures and Vink*, 2000] and the model of *Gehlen et al.* [2002]. The latter couples Al to biogenic opal with a first-order scavenging coefficient while our model represents this biological activity, scavenging, and remineralization which depend on the mass of all sinking particles (mineral dust, organic matter, biogenic silica, and calcium carbonate). This study and *Gehlen et al.* [2002] simulate realistic surface Al distributions using different dust inputs. However the vertical profiles are very different. The observed vertical profiles often have a surface maximum, a subsurface minimum, and then gradually increase with depth down to the ocean floor. *Gehlen et al.* [2002] simulate profiles with Al concentration that generally increases with depth. Our alternate approach to the scavenging and internal ocean cycling of Al tends to reproduce the observed subsurface minimum often seen in the observations (Figure S2). Considering the good surface agreement, these intermodel differences are more likely caused by physical and biological processes than by differences in the inputs from dust. Our model does lead to excessively high dissolved Al values at the ocean floor (bottom cell on the model grid) because all Al sinking on particles is remineralized at the bottom. In reality, much of this Al is likely incorporated into the sediments.

3.3. Estimated Residence Time

[20] The residence time of surface ocean dissolved Al is the ratio of total surface layer Al to the rate of input or removal. In this case, we use the sum of Al from dissolved dust plus sources due to advection and mixing as the input rate for the upper 50 m. BEC predicts surface Al residence times ranging from months to 73 years (Figure 7), consistent with previous estimates [*Orians and Bruland*, 1986; *Maring and Duce*, 1987; *Moran et al.*, 1992; *Gehlen et al.*, 2003]. Short residence times occur in high-dust areas (e.g., the equatorial Atlantic) and areas with relatively high biological activity (e.g., the equatorial Pacific). Long residence times are associated with low dust input and low biological activity as occurs in polar regions and midlatitude gyres (where there are fewer particles available to scavenge Al). The long residence times in some polar regions may be unrealistically high since the model includes no biological activity under the sea ice, thus no biological particles are available to scavenge Al in permanently ice-covered areas. In reality there is some biological production of particles within and just below the sea ice, and there also may be particles released from ice-rafted debris accumulated on or near the continent. The wide variation in residence times indicates that the BEC model could improve Al predictions (e.g., from MADCOW) by allowing the residence time to vary. The mean Al residence time of the surface ocean (0–50 m) and the whole ocean are 2.3 and 53 years, respectively.

[21] Particle scavenging and biological uptake by diatoms are the only Al removal processes. In our model, surface Al scavenging dominates the removal processes over more than 75% of the surface ocean. In the North Atlantic the

model-predicted scavenging can be 1000 times more efficient than uptake. Biological uptake significantly exceeds scavenging where silica production is high and dust flux is low, e.g., the equatorial Pacific. In this region, *Dymond et al.* [1997] found that essentially all of the sinking particulate Al was correlated with sinking opal. This suggests a dominant role for diatoms in Al removal in this region. Such regions account for <10% of the surface ocean. In other regions, scavenging and biological uptake are of similar magnitude. Globally biological uptake accounts for 30% of dissolved Al removal from the upper 50m, but particle scavenging is the only removal term below the euphotic zone.

3.4. Time Series

[22] The only sites where seasonal cycle data exist for multiple years are HOT (station ALOHA, 2245′N, 158°W) and BATS (Hydrostation S, 3210′N, 6430′W). The predicted Al seasonal cycle amplitude is weaker than observed at BATS and essentially nonexistent at HOT, although the dust deposition varies significantly with season at both sites (Figure 8). The modeled and observed Al concentrations at BATS show similar trends, and both lag the local dust deposition peak by about two months.

[23] *Johnson et al.* [2003] measured a surface Al concentration of 3nM lower than the Hawaii Ocean Time-series measurements plotted in Figure 8, and even these low-end observations are much higher than the BEC-predicted Al concentrations at HOT. *Johnson et al.* [2003] also found the inconsistency between the surface water aluminum and iron and the expected aerosol concentrations. They suggested a combined effect of higher solubility and higher aerosol scavenging rates (higher dust deposition rate) than generally assumed. Air mass back-trajectories indicate that the air over HOT often originates from within the Asian dust plume that crosses the North Pacific at higher latitudes [*Boyle et al.*, 2005]. Thus, dust deposition may be higher than predicted. Higher than model-predicted dust deposition near HOT are also sometimes observed [*McNaughton et al.*, 2006; *Buck et al.*, 2006]. In the observations the region around Hawaii stands out with elevated Al concentrations relative to waters to the east and west (Figure 6). Experiment solubility data suggest that our assumed 5% solubility is fairly applicable at HOT [*Sato*, 2003; *Buck et al.*, 2006]. This suggests that 10 times more than model-predicted dust deposition at HOT is necessary if we keep this same solubility, while the observed dust deposition flux at Oahu shows that DEAD underestimates dust deposition by only a factor of 2 [*Zender et al.*, 2003]. This discrepancy remains unresolved.

3.5. BEC Model-Data Inferred Dust Deposition (Improved MADCOW Approach)

[24] If we assume dissolved Al is in steady state, then the observed Al concentration (Figure 3a), modeled mixed layer depth (not shown) and modeled surface Al residence time (Figure 7) define an inferred dust deposition (Figure 9a). This method applies the MADCOW model but relaxes the assumptions of constant mixed layer depth and residence time. The deposition inferred from observed Al is only semi-independent of the modeled dust deposition since the

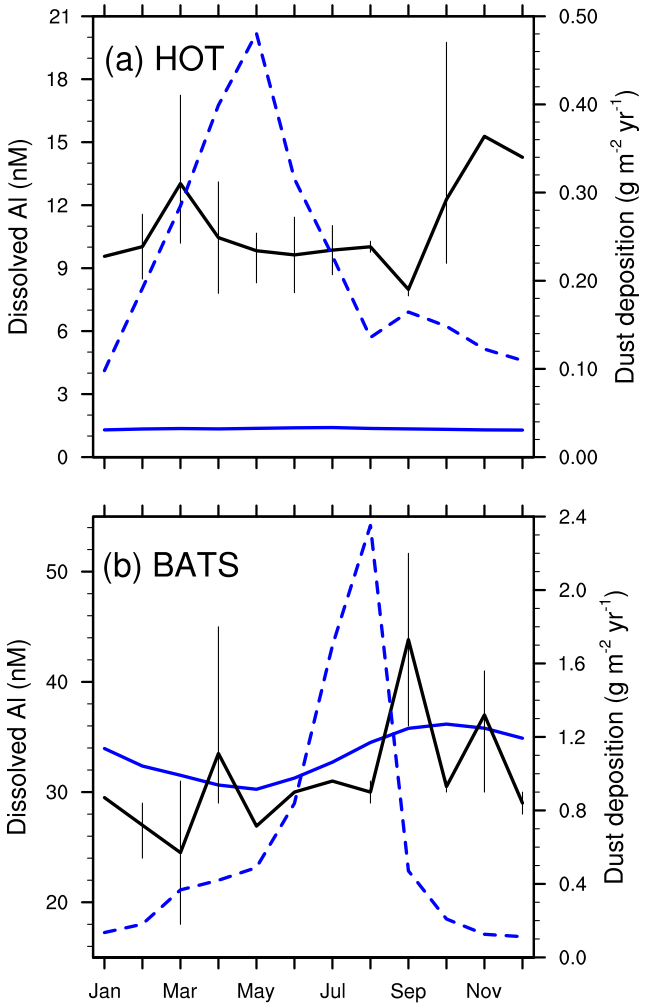

Figure 8. Observed (solid) and modeled (solid blue) Al seasonal cycle (0–50 m) at (a) HOT (C. Measures, unpublished data, 1994–1997) and (b) BATS [*Jickells*, 1986] on left-hand axis. Dust deposition (dashed) on right-hand axis. Whiskers span maximum/minimum observations when multiple years of measurements are available. No whiskers indicates only 1 year of measurements.

Al residence time is derived from the BEC model which uses the DEAD modeled dust deposition. The solubility and Al:dust weight ratio were assumed to be 5% and 8%, respectively. The inferred dust deposition shows that the current DEAD model has overestimated dust deposition at the north equatorial Atlantic but underestimated in other Atlantic regions, the Southern Ocean and the Arabian Sea. However, since the Al residence time is sensitive to the assumed Al solubility (see following section), solubility may also contribute to the mismatch between the inferred dust and DEAD simulated deposition.

4. Discussion

[25] Though we have greatly expanded the Al database, the spatial coverage is still not enough to fully understand the global Al climatology. Some regions, such as the eastern

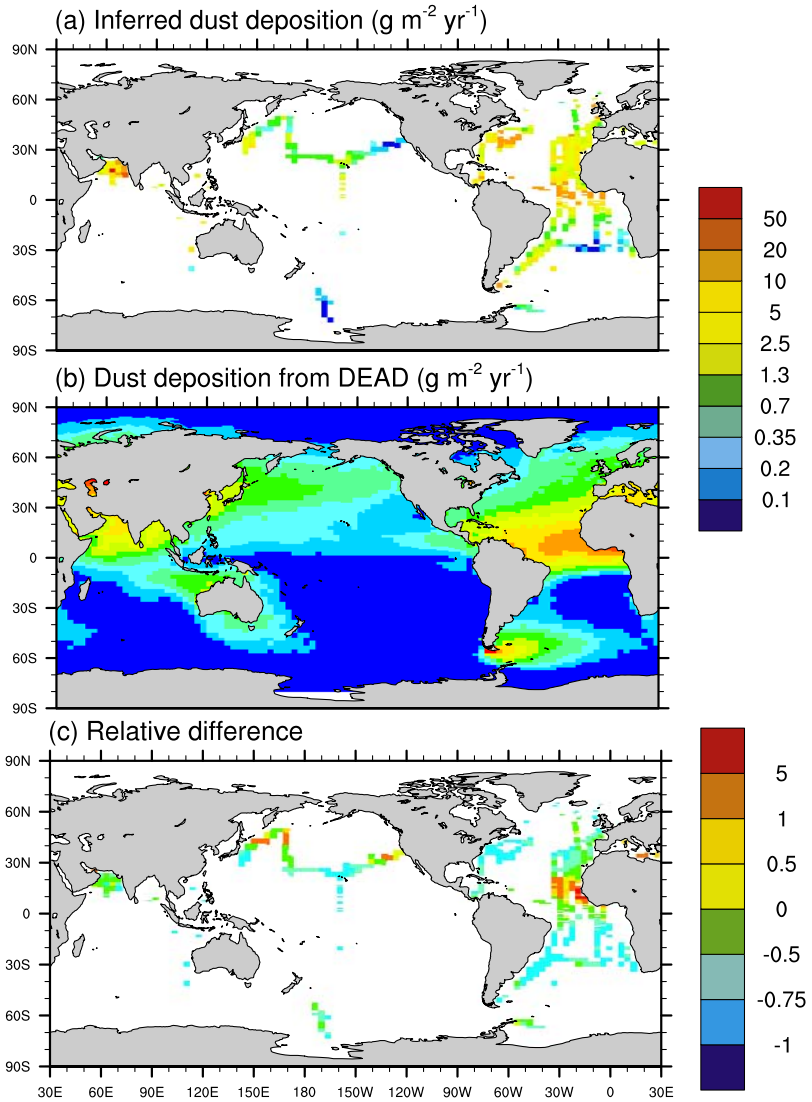

Figure 9. (a) Dust deposition field inferred from observed surface ocean Al concentration and BEC (improved MADCOW). (b) Dust deposition predicted by DEAD using observed 1990s meteorology. (c) Relative difference: (DEAD-Inferred)/Inferred.

Atlantic, have sufficient data for detailed comparisons with the model. The temporal coverage is even poorer. We have only one or two months data at most measurement locations. These few data determine the annual mean for purposes of model comparison. Since dust input to the surface ocean is highly episodic, the lack of temporal coverage might bias the derived annual mean values. At HOT and BATS, this bias can exceed 30% of the annual means on the basis of the observed seasonality (Figure 8). Interannual dust deposition variability could also exceed 30% on the basis of the observations at these sites. For regions with a longer Al residence time than HOT and BATS, this bias is acceptable, while for regions with shorter Al residence time, the bias would be larger. Also, we do not know the atmospheric conditions when the observation sample were taken. If there were a big dust event just before the ship sampling, the biases could be even larger. However, the observations display a regional coherence, with similar Al values, suggesting there were no such huge biases. The number of Al observations worldwide will increase dramatically in the coming decade because of new field campaigns, especially the basin transects associated with the CLIVAR and GEOTRACES programs.

[26] Though the model generally agrees well with the observations, there are still large discrepancies in some regions. These discrepancies could be explained by either an unrealistic input dust flux or the model parameters we choose. While the Al:dust ratio is relatively invariable, Al solubility ranges widely from 0.5% to 86% with a mean near 5% [*Prospero et al.*, 1987; *Sato*, 2003; *Baker et al.*, 2006]. *Gehlen et al.* [2003] estimate mean Al solubility is 1.5 to 3% on the basis of numerical experiment with varying solubility to minimize model measurement discrepancies. Our control run used a global uniform solubility of 5%.

[27] To investigate the model sensitivity to the model parameterizations, we first repeated the last 72 years of the

Table 3. Sensitivity Test[a]

Model Description	Surface Al Concentration (nM), 0–50 m				Residence Time (years), 0–50 m	rmsd
	Global	North Atlantic	South Atlantic	Equatorial Atlantic		
Observations		23.55	15.76	29.74		
Control run (S = 5%, r = 0.077)	8.0	33.56	15.33	55.52	2.31	0.9032
Low solubility (S = 2.5%, r = 0.077)	4.8	18.90	8.56	30.41	1.89	0.9648
High scavenge (S = 5%, r = 0.085)	7.8	32.56	14.82	53.77	2.28	0.9039
Low scavenge (S = 5%, r = 0.069)	8.9	35.83	16.36	57.69	2.71	0.9245

[a]S: solubility; r: scavenging rate(a^{-1}); rmsd: root mean square difference (after logarithm transformation). North Atlantic: the Atlantic at north of the equator; South Atlantic: the Atlantic at south of the equator; equatorial Atlantic: 0–25°N, 0–40°W.

control run with the same scavenging ratio but cutting the solubility by half. Comparing the Al concentrations between the control run and the sensitivity run, the model is highly sensitive to the solubility (Table 3). With the solubility reduced by 50%, the low-solubility run corrected the overestimation in the equatorial Atlantic region (0–25°N, 0–40°W) where the dust deposition is very high. However, all the other regions including other Atlantic areas, the Pacific and the Southern Ocean were underestimated by the low-solubility run. This result is consistent with recent findings that the solubility of Al from Saharan dust (median value 3.0%) is significantly lower than Al solubility from non-Saharan source regions (median value 9.0%) [*Baker et al.*, 2006]. Measurements and theoretical considerations also suggest that solubility will vary regionally [*Prospero et al.*, 1987; *Sato*, 2003; *Baker et al.*, 2006] and as a function of air mass history and chemical transformation [*Luo et al.*, 2005].

[28] We then repeated the last 40 years of the control run with the same solubility but changing the base scavenging rate by ±10%. Comparing the Al concentrations again between the control run and the sensitivity runs, the model is not overly sensitive to the chosen scavenging rate. Our base scavenging rate was chosen to minimize the model-data differences. Additional field observations in coming years will further constrain this Al removal term.

[29] The observed Al concentrations show clear basin-scale difference and indicate that Al is a good tracer for estimating dust deposition. We have improved the Al predictions and dust deposition estimations by using a global BEC model with dynamic mixed layer depth and Al residence time. The sensitivity test shows that the model is sensitive to Al solubility. The spatial variation of Al solubility could be an important reason for the model observation discrepancies and should be resolved in future research. Future simulations could include a spatially varying solubility based on source region and aerosol composition, aerosol size distributions, and/or distance from the source region. Observations of aerosol Al and Fe solubility are also being made on the CLIVAR cruises and will help constrain the solubility in the future. Remaining model-data discrepancies can then be attributed mainly to errors in the simulated dust deposition.

Appendix A: Al Model Description

[30] We added dissolved Al as a tracer to BEC following the parameterization for iron [*Moore and Braucher*, 2008]. The only Al source to the ocean is partial dissolution from dust deposition and the only loss from the ocean is scavenging. For the whole ocean together:

$$\frac{d[Al_{diss}]}{dt} = DISS - SCAV \times r \quad (A1)$$

where $[Al_{diss}]$ is dissolved Al concentration (mmol m^{-3}), DISS is partial dissolution of Al from dust deposition (mmol m^{-3} s^{-1}), SCAV is scavenging of Al (mmol m^{-3} s^{-1}), and r is fraction of scavenged Al assumed lost to ocean sediments, currently 20%.

[31] Al reaches the deep ocean in sinking dust, by remineralization of production and previous scavenging, and by circulation and mixing. For each layer,

$$\frac{d[Al_{diss}]}{dt} = DISS + REMIN + CIRC - PROD - SCAV \quad (A2)$$

where REMIN is Al released from remineralization from PROD and part of SCAV(80%), CIRC is Al transported by circulation and mixing, and PROD is biouptake Al.

[32] The dust deposition field can be from any observations or model predictions. Currently we use 1990s dust climatology from the DEAD model [*Zender et al.*, 2003]. Deposited dust at the surface partially dissolves immediately into the mixed layer:

$$DISS = S \times (r_{Al} \times F_{d0}) \quad (A3)$$

where S = 5% is the solubility of dust at surface ocean, r_{Al} = 8% is Al dust fraction by weight, and F_{d0} is the flux of dust at surface which comes from the dust deposition field.

[33] As dust particles sink they keep dissolving and cause another ~6% dissolution of Al throughout the ocean:

$$DISS = r_{Al} \times [(F_{ds\_in} - F_{ds\_out}) + (F_{dh\_in} - F_{dh\_out})] \quad (A4)$$

where F_{ds_in} and F_{dh_in} are soft (defined as easy to remineralization) or hard (defined as resistant to remineralization) dust flux coming into the layer, and F_{ds_out} and F_{ds_out} are soft or hard dust flux going out of the layer. They are derived by:

$$F_{ds\_out} = e^{-dz/L_{ds}} \times F_{ds\_in} \quad (A5a)$$

$$F_{dh\_out} = e^{-dz/L_{dh}} \times F_{dh\_in} \quad (A5b)$$

where dz is layer thickness, L_{ds} = 600 m is the dissolution length scale for soft dust fractions, and L_{dh} = 120,000 m is

the dissolution length scale for hard dust fractions. In all layers except the surface F_{ds_out} and F_{ds_out} from above equal F_{ds_in} and F_{dh_in} to the next layer. At the surface:

$$F_{ds\_in} = (1 - S) \times (1 - \mathrm{f_{hd}}) \times F_{d0} \tag{A6a}$$

$$F_{dh\_in} = (1 - S) \times \mathrm{f_{hd}} \times F_{d0} \tag{A6b}$$

where $\mathrm{f_{hd}}$ = 97% is the hard fraction of dust flux.

[34] Remineralization of Al depends on POC remineralization:

$$\mathrm{REMIN} = \mathrm{REMIN_{POC}} \times \frac{F_{Al\_in}}{(F_{POCs\_in} + F_{POCh\_in})} \tag{A7}$$

where the notation and conventions for (A6b) have been applied to soft and hard POC. F_{Al_in} is the particle Al flux coming into the layer. The flux F_{Al_in} are zero at the surface, while beneath the surface equals the outgoing flux F_{Al_out} from the above layer. The outgoing Al flux is defined as:

$$F_{Als\_out} = F_{Als\_in} + \mathrm{PROD} + 80\% \times \mathrm{SCAV} - \mathrm{REMIN} \tag{A8}$$

[35] In the data *Gehlen et al.* [2002] reported, we found an approximate relation among biouptake Al, biouptake Si, dissolved Al and dissolved Si:

$$\frac{\mathrm{PROD}}{P_{Si}} = \mathrm{C_1} \times \frac{[\mathrm{Al_{diss}}]}{[\mathrm{Si_{diss}}]} \tag{A9}$$

where $\mathrm{C_1}$ = 0.08845 is a constant. To avoid overflow, we set $P_{Si} \geq 0.1$ mmol $\mathrm{m^{-3}}$.

[36] Scavenging is the dominant process that removes dissolved Al. We model scavenging as proportional to the dissolved Al concentration

$$\mathrm{SCAV} = r_{scav} \times [\mathrm{Al_{diss}}] \tag{A10}$$

where r_{scav} is the scavenging rate and is determined by the surrounding particle concentration (including POC, $CaCO_3$, SiO_2 and dust)

$$r_{scav} = \mathrm{r_{scav\_base}} \times (F_{POC} \times \mathrm{C_2} + F_{CaCO_3} \times \mathrm{C_3} + F_{SiO_2} \times \mathrm{C_4} + F_d \times \mathrm{C_5}) \tag{A11}$$

where $\mathrm{r_{scav\_base}} = 0.077\ a^{-1}$ is the base rate, we choose this rate to make the model results best fit the observations; $\mathrm{C_2}$, $\mathrm{C_3}$, $\mathrm{C_4}$, $\mathrm{C_5}$, are scaling factors, F_{POC} is POC flux, F_{CaCO3} is $CaCO_3$ flux, F_{SiO2} is SiO_2 flux, and F_d is dust flux.

References

Andersen, K. K., A. Armengaud, and C. Genthon (1998), Atmospheric dust under glacial and interglacial conditions, *Geophys. Res. Lett.*, *25*(13), 2281–2284.

Armstrong, R. A., C. Lee, J. I. Hedges, S. Honjo, and S. G. Wakeham (2002), A new, mechanistic model for organic carbon fluxes in the ocean based on the quantitative association of poc with ballast minerals, *Deep Sea Res., Part II*, *49*, 219–236.

Baker, A. R., T. D. Jickells, M. Witt, and K. L. Linge (2006), Trends in the solubility of iron, aluminium, manganese and phosphorus in aerosol collected over the Atlantic Ocean, *Mar. Chem.*, *98*, 43–58.

Bowie, A. R., D. J. Whitworth, E. P. Achterberg, R. F. C. Mantoura, and P. J. Worsfold (2002), Biogeochemistry of Fe and other trace elements (Al, Co, Ni) in the upper Atlantic Ocean, *Deep Sea Res., Part I*, *49*, 605–636.

Boyle, E. A., B. A. Bergquist, R. A. Kayser, and N. Mahowald (2005), Iron, manganese and lead at Hawaii Ocean Time-series station ALOHA: Temporal variability and an intermediate water hydrothermal plume, *Geochim. Cosmochim. Acta*, *69*(4), 933–952.

Brown, E. T., C. I. Measures, J. M. Edmond, D. L. Bourles, G. M. Raisbeck, and F. Yiou (1992), Continental inputs of beryllium to the oceans, *Earth Planet. Sci. Lett.*, *114*, 101–111.

Bruland, K. W., and M. C. Lohan (2003), Controls of trace metals in seawater, in *Treatise on Geochemistry*, pp. 23–47, Elsevier, New York.

Buck, C. S., W. M. Landing, J. A. Resing, and G. T. Lebon (2006), Aerosol iron and aluminum solubility in the northwest Pacific Ocean: Results from the 2002 IOC cruise, *Geochem. Geophys. Geosyst.*, *7*, Q04M07, doi:10.1029/2005GC000977.

Caschetto, S., and R. Wollast (1979), Vertical distribution of dissolved aluminium in the Mediterranean Sea, *Mar. Chem.*, *7*, 141–155.

Chou, L., and R. Wollast (1997), Biogeochemical behavior and mass balance of dissolved aluminum in the western Mediterranean Sea, *Deep Sea Res., Part II*, *44*(34), 741–768.

Collins, W. D., et al. (2006), The community climate system model version3 (CCSM3), *J. Clim.*, *19*(11), 2122–2161.

Doney, S. C., K. Lindsay, and J. K. Moore (2003), Global ocean carbon cycle modeling, in *Ocean Biogeochemistry: The Role of the Ocean Carbon Cycle in Global Change*, edited by M. J. R. Fashom et al., pp. 217–238, Springer, Berlin.

Duce, R. A., et al. (1991), The atmospheric input of trace species to the world ocean, *Global Biogeochem. Cycles*, *5*(3), 193–259.

Dymond, J., R. Collier, J. McManus, S. Honjo, and S. Manganini (1997), Can the aluminum and titanium contents of ocean sediments be used to determine the paleoproductivity of the oceans, *Paleoceanography*, *12*(4), 586–593.

Fung, I. Y., S. K. Meyna, I. Tegen, S. C. Doney, J. G. John, and J. K. B. Bishop (2000), Iron supply and demand in upper ocean, *Global Biogeochem. Cycles*, *14*(1), 281–295.

Gehlen, M., L. Beck, G. Calas, A. M. Flank, A. J. Van Bennekom, and J. E. E. Van Beusekom (2002), Unraveling the atomic structure of biogenic silica: Evidence of the structural association of Al and Si in diatom frustules, *Geochim. Cosmochim. Acta*, *66*(9), 1601–1609.

Gehlen, M., C. Heinze, E. Maier-Reimer, and C. I. Measures (2003), Coupled Al-Si geochemistry in an ocean general circulation model: A tool for the validation of oceanic dust deposition fields?, *Global Biogeochem. Cycles*, *17*(1), 1028, doi:10.1029/2001GB001549.

Ginoux, P., M. Chin, I. Tegen, J. M. Prospero, B. Holben, O. Dubovik, and S. Jiann Lin (2001), Sources and distributions of dust aerosols simulated with the Gocart model, *J. Geophys. Res.*, *106*, 20,255–20,273.

Hall, I. R., and C. I. Measures (1998), The distribution of Al in the IOC stations of the North Atlantic and Norwegian Sea between 52 and 65 north, *Mar. Chem.*, *61*, 69–85.

Helmers, E., and M. M. R. van der Loeff (1993), Lead and aluminum in Atlantic surface waters (50N to 50S) reflecting anthropogenic and natural sources in the eolian transport, *J. Geophys. Res.*, *98*, 20,261–20,274.

Hydes, D. J. (1979), Aluminum in seawater: Control by inorganic processes, *Science*, *205*(4412), 1260–1262.

Hydes, D. J. (1983), Distribution of aluminium in waters of the north east Atlantic 25N to 35N, *Geochim. Cosmochim. Acta*, *47*(5), 967–973.

Hydes, D. J., and P. S. Liss (1976), Fluorimetric method for the determination of low concentrations of dissolved aluminium in natural waters, *Analyst*, *101*, 922–931.

Hydes, D. J., G. J. D. Lange, and H. J. W. D. Baar (1988), Dissolved aluminium in the Mediterranean, *Geochim. Cosmochim. Acta*, *52*(8), 2107–2114.

Jickells, T. D. (1986), Studies of trace elements in the Sargasso Sea and the mid Atlantic Bight, Ph.D. thesis, Univ. of Southampton, Southampton, UK.

Jickells, T., T. Church, A. Veron, and R. Arimoto (1994), Atmospheric inputs of manganese and aluminium to the sargasso sea and their relation to surface water concentrations, *Mar. Chem.*, *46*, 283–292.

Johnson, K. S., et al. (2003), Surface ocean-lower atmosphere interactions in the northeast Pacific Ocean gyre: Aerosols, iron, and the ecosystem response, *Global Biogeochem. Cycles*, *17*(2), 1063, doi:10.1029/2002GB002004.

Kramer, J., P. Laan, G. Sarthou, K. R. Timmermans, and H. de Baar (2004), Distribution of dissolved aluminium in the high atmospheric input region of the subtropical waters of the North Atlantic Ocean, *Mar. Chem.*, *88*, 85–101.

Kremling, K. (1985), The distribution of cadmium, copper, nickel, manganese, and alu- minium in surface waters of the open Atlantic and European shelf area, *Deep Sea Res.*, *32*(5), 531–555.

Krishnamurthy, A., J. K. Moore, and S. C. Doney (2008), The effects of dilution and mixed layer depth on deliberate ocean iron fertilization: 1-D simulations of the Southern Ocean Iron Experiment (SOFeX), *J. Mar. Syst*, in press. (Available at http://www.ess.uci.edu/jkmoore/)

Luo, C., N. M. Mahowald, N. Meskhidze, Y. Chen, R. L. Siefert, A. R. Baker, and A. M. Johansen (2005), Estimation of iron solubility from observations and a global aerosol model, *J. Geophys. Res.*, *110*, D23307, doi:10.1029/2005JD006059.

Mahowald, N., K. Kohfeld, M. Hansson, Y. Balkanski, S. Harrison, I. C. Prentice, M. Schulz, and H. Rodhe (1999), Dust sources and deposition during the LGM and current climate: A comparison of model results with paleodata from ice cores and marine sediments, *J. Geophys. Res.*, *104*, 15,895–15,916.

Mahowald, N. M., D. R. Muhs, S. Levis, P. J. Rasch, M. Yoshioka, C. S. Zender, and C. Luo (2006), Change in atmospheric mineral aerosols in response to climate: Last glacial period, preindustrial, modern, and doubled carbon dioxide climates, *J. Geophys. Res.*, *111*, D10202, doi:10.1029/2005JD006653.

Maring, H. B., and R. A. Duce (1987), The impact of atmospheric aerosols on trace metal chemistry in open ocean surface seawater: 1. Aluminum, *Earth Planet. Sci. Lett.*, *84*, 381–392.

Martin, H. B., and S. E. Fitzwater (1988), Iron deficiency limits phyoplankton growth in the north-east Pacific subarctic, *Nature*, *331*, 341–343.

McNaughton, C., A. Clarke, V. Kapustin, J. Dibb, B. Anderson, E. Browell, and G. Carmichael (2006), Entrainment of free troposphere Asian dust/pollution into the marine boundary layer north of Hawaii during INTEX-B, *Eos Trans. AGU*, *87*(52), Fall Meet. Suppl., Abstract A53A-0150.

Measures, C. I. (1995), The distribution of Al in the IOC stations of the eastern Atlantic between 30S and 34N, *Mar. Chem.*, *49*, 267–281.

Measures, C. I., and E. T. Brown (1996), Estimating dust input to the Atlantic Ocean using surface water aluminum concentrations, in *The Impact of Desert Dusts Across the Mediterranean*, edited by S. Guerzoni and R. Chester, pp. 301–311, Springer, New York.

Measures, C. I., and J. M. Edmond (1989), Shipboard determination of aluminum in sawater at the nanomolar level by electron capture detection gas chromatography, *Anal. Chem.*, *61*, 544–547.

Measures, C. I., and J. M. Edmond (1990), Aluminium in the South Atlantic: steady state distribution of a short residence time element, *J. Geophys. Res.*, *95*, 5331–5340.

Measures, C. I., and S. Vink (1999), Seasonal variations in the distribution of Fe and Al in the surface waters of the Arabian Sea, *Deep Sea Res., Part II*, *46*, 1597–1622.

Measures, C. I., and S. Vink (2000), On the use of dissolved aluminum in surface waters to estimate dust deposition to ocean, *Global Biogeochem. Cycles*, *14*(1), 317–327.

Measures, C. I., B. Grant, M. Khadem, D. S. Lee, and J. M. Edmond (1984), Distribution of Be, A1, Se and Bi in the surface waters of the western North Atlantic and Caribbean, *Earth Planet. Sci. Lett.*, *71*, 1–12.

Measures, C. I., J. M. Edmond, and T. D. Jickells (1986), Aluminium in the northwest Atlantic, *Geochim. Cosmochim. Acta*, *50*(7), 1423–1429.

Measures, C. I., M. T. Brown, and S. Vink (2005), Dust deposition to the surface wa- ters of the western and central North Pacific inferred from surface water dissolved aluminum concentrations, *Geochem. Geophys. Geosyst.*, *6*, Q09M03, doi:10.1029/2005GC000922.

Moore, J. K., and O. Braucher (2008), Sedimentary and mineral dust sources of dissolved iron to the world ocean, *Biogeosciences*, in press.

Moore, J. K., S. C. Doney, J. A. Kleypas, D. M. Glover, and I. Y. Fung (2002), An intermediate complexity marine ecosystem model for the global domain, *Deep Sea Res., Part II*, *49*, 403–462.

Moore, J. K., S. C. Doney, and K. Lindsay (2004), Upper ocean ecosystem dynamics and iron cycling in a global three-dimensional model, *Global Biogeochem. Cycles*, *18*, GB4028, doi:10.1029/2004GB002220.

Moore, J. K., S. C. Doney, K. Lindsay, N. Mahowald, and M. Anthony (2006), Nitrogen fixation amplifies the ocean biogeochemical response to decadal timescale variations in mineral dust deposition, *Tellus, Ser. B*, *58*, 560–572.

Moran, S. B., R. M. Moore, and S. Westerlund (1992), Dissolved aluminum in the Weddell Sea, *Deep Sea Res., Part A*, *39*(3/4), 537–547.

Narvekar, P. V., and S. Y. S. Singbal (1993), Dissolved aluminium in the surface microlayer of the eastern Arabian Sea, *Mar. Chem*, *42*, 85–94.

Obata, H., Y. Nozaki, D. S. Alibo, and Y. Yamamoto (2004), Dissolved Al, In, and Ce in the eastern Indian Ocean and the Southeast Asian seas in comparison with the ra- dionuclides 210Pb and 210Po, *Geochim. Cosmochim. Acta*, *68*(5), 1035–1048, doi:10.1016/j.gca.2003.07.021.

Orians, K. J., and K. W. Bruland (1985), Dissolved aluminium in the central North Pacific, *Nature*, *316*, 427–429.

Orians, K. J., and K. W. Bruland (1986), The biogeochemistry of aluminum in the Pacific Ocean, *Earth Planet. Sci. Lett.*, *78*, 397–410.

Prospero, J. M. (1996), The atmospheric transport of particles to the ocean, in *Particle Flux in the Ocean*, pp. 19–52, John Wiley, New York.

Prospero, J. M., R. T. Nees, and M. Uematsu (1987), Deposition rate of particulate and dissolved aluminum derived from saharan dust in preici-pitation at miami, florida, *J. Geophys. Res.*, *92*, 14,723–14,731.

Sanudo-Wilhelmy, S. A., K. A. Olsen, J. M. Scelfo, and T. D. F. abd A. R. Flegal (2002), Trace metal distributions off the antarctic peninsula in the Weddell Sea, *Mar. Chem.*, *77*, 157–170.

Sato, T. (2003), The fractional solubility of aluminum from atmospheric aerosols, Master's thesis, Univ. of Hawaii at Manoa, Honolulu, Hawaii.

Stoffyn, M., and F. T. Mackenzie (1982), Fate of dissolved aluminum in the oceans, *Mar. Chem.*, *11*, 105–127.

Upadhyay, S., and R. S. Gupta (1994), Aluminium in the northwestern Indian Ocean (Arabian Sea), *Mar. Chem.*, *47*, 203–214.

Vink, S., and C. I. Measures (2001), The role of dust deposition in determining surface water distributions of Al and Fe in the south west Atlantic, *Deep Sea Res., Part II*, *48*, 2787–2809.

Wedephohl, K. H. (1995), The compositon of the continental crust, *Geochim. Cosmochim. Acta*, *59*(7), 1217–1232.

Zender, C. S., H. Bian, and D. Newman (2003), Mineral Dust Entrainment and Deposition (DEAD) model: Description and 1990s dust climatology, *J. Geophys. Res.*, *108*(D14), 4416, doi:10.1029/2002JD002775.

Zender, C. S., R. L. Miller, and I. Tegen (2004), Quantifying mineral dust mass budgets: Terminology, constraints, and current estimates, *Eos Trans. AGU*, *85*(48), 509–512.

Q. Han, D. Hydes, C. Measures, J. K. Moore, and C. Zender, Department of Earth System Science, University of California, Irvine, Croul Hall, Irvine, CA 92697-3100, USA. (qhan@uci.edu)